Integrated Radar Monitoring System (IRaMS): automated nearshore observations of swimming and navigation hazards, surf conditions, and engineering parameters

Jesse McNinch and Jonathon Waddell

Executive Summary

The Integrated Radar Monitoring System (IRaMS) has been developed by USACE Detroit District (LRE) to make nearshore observations around the Great Lakes and other coastal settings. IRaMS utilizes over-the-counter hardware, namely a marine X-band radar and a single board computer, coupled with software developed in-house to measure a range of physical processes common in the nearshore environment. X-band returns a strong signal from surface gravity waves, foam, and other disturbances that roughen the water surface. IRaMS exploits this signal sensitivity to explicitly measure wave crests and other phenomena every 1-2s, over distances ranging from 0.2-3km with respective grid resolutions of 1-3m. These spatiotemporal observations are used to extract a range of wave parameters – period, speed, wavelength, breaking – and surface currents, which are then used to calculate bathymetry, wave height, and alongshore radiation stress. USACE-LRE has deployed semi-permanent IRaMS stations across all five of the Great Lakes in the past twelve months. Power at each station is sustained through a small solar panel and remotely triggered smart sampling strategies. Automated powering and data collection are triggered by user-defined thresholds from continuously updated regional wave forecasts. Compressed data files are pushed to the cloud at the conclusion of each collection. We anticipate a wealth of use from building a long, time series of observations for engineering design and model validation to identifying real-time swimming and navigation hazards as well as showing wave conditions at popular surfing breaks.

Technical Specifications

IRaMS assembles over-the-counter hardware and our proprietary software to measure waves and other phenomena on the water surface over ranges of 200m – 4km. Horizontal resolution varies as a function of range, approximately 0.002 of range. Collection duration is 5min at ~0.8Hz. These data are autonomously uploaded and pre-processed in the cloud, returning downloadable products within 5min of the observation. Next-step goals include performing all post-processing in the cloud and displaying each product as georectified maps through time.

Hardware: All hardware components – Single Board Computer, GPS puck, Radar Interface, Cellular modem, 12v battery – are assembled within a weather-proof enclosure (20x50x15cm). The two external components include a 60W solar panel and site-defined radar antenna (ranging from a dome up to a 2-meter open array). The hardware box, solar panel, and radar antenna may be mounted on a small metal pole (Figure 1) or on any available small structure located near the area of interest.

Figure 1: Pole Mounted Deployment.

Costs: hardware and assembly expenses range from $10K to $15K, depending on needed radar antenna model and the complexities of a given site location.

Software: All software was developed exclusively in-house using a single coding language, Matlab, to execute every facet of operations from hardware interfacing, data collection, and cloud uploading. We are converting the operation and in-cloud processing code to python to eliminate proprietary software licenses or agreement requirements to our stakeholders. To improve data accessibility, all cloud services are being planned for migration to the Great Lakes Observing System (GLOS), a regional associate in NOAA's Integrated Ocean Observing System, servers within the next 6-12 months. However, a simplified temporary demonstration prototype is available through Coastal Measures LLC. (link available upon request). Currently, data are uploaded from deployed IRaMS and pre-processed results are displayed in near, real-time (exemplified in Figure 2). Figure 2 shows raw radar data (left panel) and partial-processed results mapping shoals near a navigation channel. This example only demonstrates an active cloud platform that receives and displays radar data in real-time from our field systems.

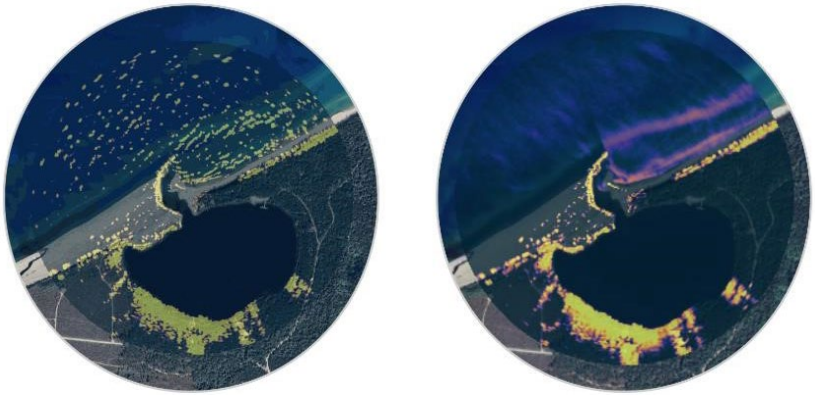

Figure 2: IRaMS cloud archiving and display

Products

Waves: The X-band radar signal, at a frequency of 9.8GHz, is particularly sensitive to water surface roughness that is often expressed in coastal settings as ripples, waves, breaking waves, ice, and foam. Simply put, we can map the water surface over 1-2km, at a grid resolution of 1-2m, every second for 5-6min from which many wave parameters may be extracted. These parameters include:

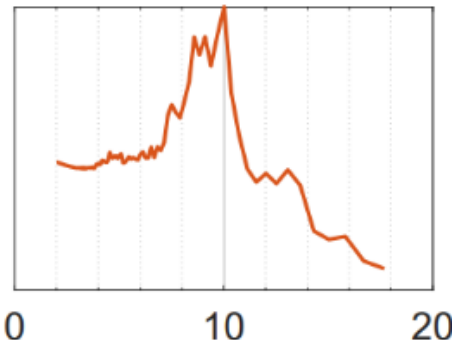

Figure 3: Wave spectra with normalized power

wave spectra at every grid node (period range 2-20s) as well as the peak frequency across the domain (Figure 3).

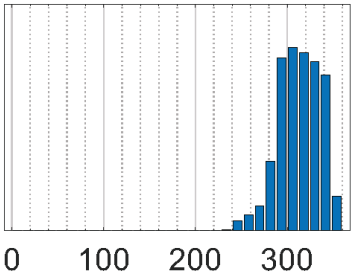

Figure 4: Histogram of wave directions across domain

wave direction measured at each node from each radar rotation in image-space which provides a time series of wave direction at 0.8Hz for five minutes across the domain (Figures 4 & 5). This methodology provides spatial and temporal measurements of wave-wave and wave-structure interactions that are very difficult to obtain using traditional in-situ gauges (Szczyrba, et. al, 2023).

wave speed and wavelength, measured explicitly in image-space, provide a time series at 0.8Hz for five minutes across the domain. This methodology enables correct pairing of the dominant period with direct measurements of wave distance traveled, giving two solutions for wave speed at each grid node.

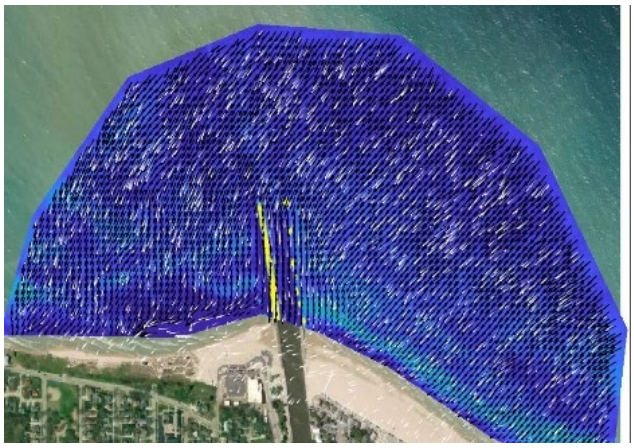
Figure 5: Map view of wave velocity vectors at each grid node

wave heights are calculated from explicit measures of wave period and wavelength to determine wave number. A fitted planar slope across the domain, using depths determined from measures of wave speed, is created to identify intermediate and shallow-water waves. Stokes Second-order equation is then employed to iteratively solve for the heights of intermediate waves while Green's law is used to determine height for shallow-water waves (Figure 6).

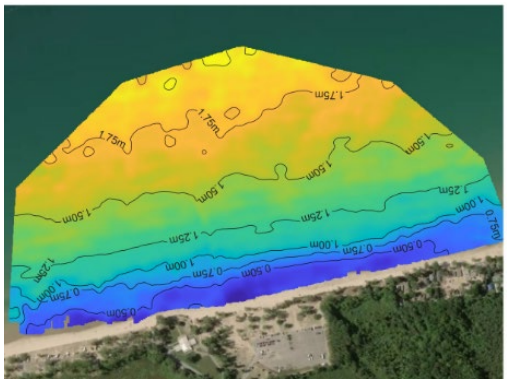

Figure 6: Map view of color mapped wave heights across the domain (m).

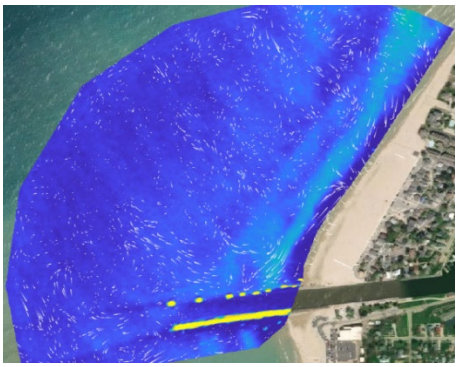

Figure 7: Map view of particle traced surface current vectors

Currents: surface currents are measured by tracking the motion of persistent water-surface roughness - after removing waves and other phenomena occurring in the incident band (<20s). This approach often reveals the presence of rip currents and other nearshore circulation currents that are expressed at the water surface (Figure 7).

Radiation stress calculated in the alongshore direction provides a measure of force, in Joules per square meter, of wave-driven currents that may transport sediment. Persistent regions of converging radiation stress may lead to deposition on sandbars and accretion on adjacent shoreline; conversely, diverging regions may lead to shoreline erosion (Figure 8).

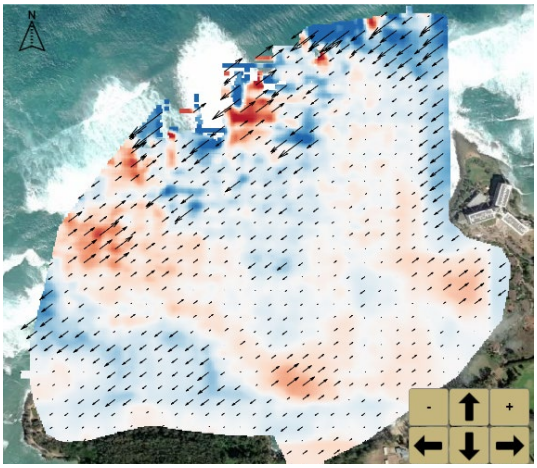

Figure 8: Map view of color mapped alongshore radiation stress with vectors.

Bathymetry: Depths at every grid cell are calculated from measured wave speed and wave period using an inversion of the linear dispersion equation (Oades, et. al., 2023; Matthijs et al., 2020). Obtaining measures of wave speed and period from each image at every grid node provides hundreds of depth solutions from each 5-min collection which enables robust statistical filters to identify errors and only use values of higher precision (Figure 9).

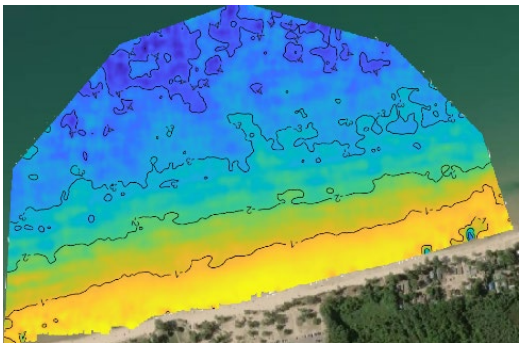

Figure 9: Map view of depths (m) shown as color drape and contours.

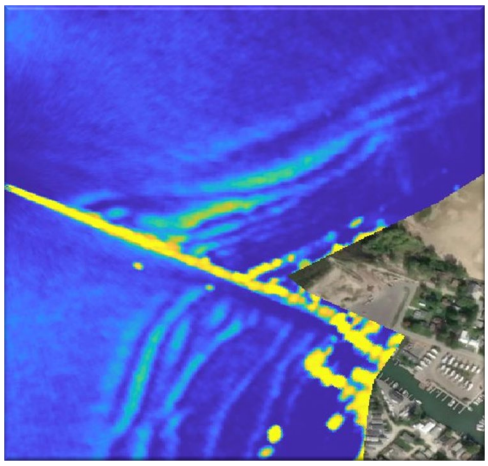

Figure 10: Map view of sand shoals near a jetty at Caseville, MI. The warmer colors show the shape and location of sand shoals encroaching the navigation channel.

Shoal and sandbar location and shape, as well as shoal migration over time, is mapped from measures of persistent wave shoaling and breaking (McNinch, 2007; Rogowski et al., 2018). These observations are often useful in interpreting the pathways and direction of sand-size sediment transport, as well as forecasting when and where shoals may encroach navigation channels (Figure 10).

Execution time: all product solutions may be completed within 5min of data collection. Processing algorithms have been optimized to perform directly on either the IRaMS-field single board computer or a cloud server.

Accuracy: The accuracy and precision of each of the products depend largely on the waves present at the time of data collection. Solutions obtained from waves that are either too small in height and/or too short in period are often erroneous because they are poorly mapped by the radar and do not align well with the assumptions in linear wave theory. When intermediate and shallow-water waves are present and captured within the IRaMS domain, accuracy falls within +- 10-15% of independently measured depths and wave parameters (Oades, et. al., 2023; Matthijs et al., 2020). IRaMS utilizes an autonomous, smart sampling strategy that reduces erroneous results by only collecting data when wave conditions are more optimal for these product solutions as well as filtering regions that do not satisfy precision thresholds.

References

Matthijs, G., et. al., 2020, The application of a radar-based depth inversion method to monitor near-shore nourishments on an open sandy coast and an ebb-tidal delta, Coastal Engineering, Volume 159,103716,ISSN 0378-3839.

McNinch, J. 2007, Bar and Swash Imaging Radar (BASIR): A Mobile X-band Radar Designed for Mapping Nearshore Sand Bars and Swash-Defined Shorelines Over Large Distances, *Journal of Coastal Research* (2007) 23 (1 (231)): 59–74.

Oades, E.M. et al., 2023, Evaluation of nearshore bathymetric inversion algorithms using camera observations and synthetic numerical input of surface waves during storms, Coastal Engineering, Volume 184, 104338, ISSN 0378-3839.

Rogowski, P. et. al., 2018, X-Band Radar Mapping of Morphological Changes at a Dynamic Coastal Inlet, Journal of Geophysical Research Earth Surfaces, Vol. 123, Issue 11, p. 3034-3054.

Szczyrba, L, et. al., 2023, Nearshore wave angles and directional variability during storm events, *Coastal Engineering*, Volume 185, 104372, ISSN 0378-3839.